NeuroImage 106 (2015) 144–153

Contents lists available at ScienceDirect

NeuroImage

journal homepage: www.elsevier.com/locate/ynimg

Effective connectivity within the frontoparietal control network differentiates cognitive control and working memory

Ian H. Harding [a,b,*], Murat Yücel [b], Ben J. Harrison [a], Christos Pantelis [a], Michael Breakspear [c,d]

[a] Melbourne Neuropsychiatry Centre, Department of Psychiatry, University of Melbourne & Melbourne Health, Melbourne, Australia
[b] Monash Clinical and Imaging Neuroscience, School of Psychological Sciences, Monash University, Melbourne, Australia
[c] QIMR Berghofer Medical Research Institute, Brisbane, QLD, Australia
[d] Metro North Mental Health Service, Brisbane, QLD, Australia

ARTICLE INFO

Article history:
Accepted 18 November 2014
Available online 22 November 2014

Keywords:
Cognitive control
Working memory
Dynamic causal modeling
Frontoparietal
Effective connectivity

ABSTRACT

Cognitive control and working memory rely upon a common fronto-parietal network that includes the inferior frontal junction (IFJ), dorsolateral prefrontal cortex (dlPFC), pre-supplementary motor area/dorsal anterior cingulate cortex (pSMA/dACC), and intraparietal sulcus (IPS). This network is able to flexibly adapt its function in response to changing behavioral goals, mediating a wide range of cognitive demands. Here we apply dynamic causal modeling to functional magnetic resonance imaging data to characterize task-related alterations in the strength of network interactions across distinct cognitive processes. Evidence in favor of task-related connectivity dynamics was accrued across a very large space of possible network structures. Cognitive control and working memory demands were manipulated using a factorial combination of the multi-source interference task and a verbal 2-back working memory task, respectively. Both were found to alter the sensitivity of the IFJ to perceptual information, and to increase IFJ-to-pSMA/dACC connectivity. In contrast, increased connectivity from the pSMA/dACC to the IPS, as well as from the dlPFC to the IFJ, was uniquely driven by cognitive control demands; a task-induced negative influence of the dlPFC on the pSMA/dACC was specific to working memory demands. These results reflect a system of both shared and unique context-dependent dynamics within the fronto-parietal network. Mechanisms supporting cognitive engagement, response selection, and action evaluation may be shared across cognitive domains, while dynamic updating of task and context representations within this network are potentially specific to changing demands on cognitive control.

Introduction

Cognitive control (CC) and working memory (WM) rely on neural processing within a common set of brain regions encompassing dorsomedial prefrontal, lateral prefrontal, and superior parietal regions of the human cortex (Fedorenko et al., 2013; Harding et al., in press; Niendam et al., 2012). This so-called "frontoparietal network" (FPN) represents a flexible, superordinate system supporting adaptive behavioral control across a broad range of cognitive demands (Cocchi et al., 2013; Cole et al., 2013; Dosenbach et al., 2008). The inherent flexibility of this system has been linked to rapid adjustments in neuronal response profiles as a function of changing behavioral goals or contextual cues (Kadohisa et al., 2013; Stokes et al., 2013). However, the neural mechanisms underlying such dynamic representation of unique behavioral goals and encoding of diverse contextual information remain unclear.

Functional neuroimaging research has established that activity in the regions forming the FPN demonstrate temporal coherence (i.e., functional connectivity) in human subjects at rest (Cole and Schneider, 2007; Power et al., 2011). The magnitude of these intrinsic inter-regional interactions has additionally been shown to selectively change in response to behavioral demands, as demonstrated most clearly in studies exploring the dynamic interplay between the dorsomedial and dorsolateral prefrontal cortices during cognitive control tasks (Carter and van Veen, 2007; Prado et al., 2011; Stephan et al., 2003).

More recently, research has moved beyond the study of FPN connectivity using pair-wise correlations in brain signals, employing techniques that are sensitive to network-wide and directional interdependencies (i.e., effective connectivity; Friston, 2011). Dynamic causal modeling (DCM) provides one means to infer neural interactions and their task-dependent changes within a brain network (Friston et al., 2003). In contrast to alternative effective connectivity modeling approaches (e.g., Structural Equation Modeling), DCM models dynamics at the level of neuronal populations, as opposed to the measured hemodynamics, providing greater construct validity to derived models of network function (Daunizeau et al., 2011). Moreover, DCM does not depend on the temporal precedence of one regional time series relative to another (as in

* Corresponding author at: School of Psychological Sciences, Building 17, Clayton Campus, Monash University, VIC 3800, Australia. Fax: +61 3 9348 0469.
E-mail address: ian.harding@monash.edu (I.H. Harding).

http://dx.doi.org/10.1016/j.neuroimage.2014.11.039
1053-8119/

multivariate autoregressive models); reliance on temporal lag may be problematic to inference using fMRI data (Friston et al., 2013).

Studies employing DCM to explore the FPN have identified sparse task-related connectivity dynamics on top of a foundation of widespread task-invariant "baseline" interactions, largely mirroring correlation-based work (Cieslik et al., 2011; Fan et al., 2008; Schlosser et al., 2008; Wang et al., 2010). In particular, Schlosser et al. (2010) report modulations of medial–lateral prefrontal interactions during performance of a Stroop task, while WM load has been associated with the transient gating of, primarily, fronto-parietal connectivity (Deserno et al., 2012; Dima et al., 2014; Ma et al., 2012; Schmidt et al., 2014). These findings point to a well-integrated network whose interactions are selectively weighted in response to current behavioral demands, reflecting a potential mechanism of adaptive coding within the FPN (Duncan, 2001). However, dissimilar experimental protocols and definitions of the FPN across available investigations preclude a more unified account of the response of this network across different cognitive domains.

Here we utilize DCM to investigate task-related changes in the FPN as CC and WM demands are systematically co-varied within a single fMRI task. Task-related dynamics of the interactions between the visual system and the FPN are first explored to assess the shared versus unique mechanisms underlying the selective engagement of higher-order cognitive processes. Context-dependent plasticity between the major regions of the FPN as a function of CC or WM demands is then assessed to distinguish their relative contributions to underlying connectivity dynamics.

Materials & methods

Participants

Twenty-five right-handed healthy adults (14 males; mean age ± s.d. = 25.5 ± 4.4 years) with no history of psychiatric or neurologic illness were recruited from the general community through advertisements in local electronic media. Exclusion criteria included a history of psychiatric or neurologic illness, substance dependence, significant head injury, current use of psychotropic medications, or MRI incompatibility (e.g., cardiac pace-maker), as assessed using the Structured Clinical Interview for DSM-IV Axis-I Disorders (First et al., 2002) and self-report. Participants had completed an average of 14.8 ± 2.2 years of education and had a mean estimated full-scale IQ of 110 ± 10 (Wechsler Abbreviated Scale of Intelligence; Wechsler, 1999). This participant sample is the same as that reported in Harding et al. (in press). The local research and ethics committee approved study conduct and all participants provided written informed consent.

Behavioral paradigm

CC and WM demands were respectively manipulated using the multi-source interference task (MSIT; Bush and Shin, 2006) and a verbal *n*-back working memory task ($n = 0$, 1, or 2; Baddeley, 2003), combined in a 2×3 factorial design. This design allowed for orthogonal manipulation of CC and WM demands within a common task context. As illustrated in Fig. 1, and described in full detail elsewhere (Harding et al., in press), participants were presented with sets of three numbers ranging in value from '0' to '3', with one number distinct to the other two (e.g., '2 1 1'), and instructed to identify the distinct number by button press ('1' = index; '2' = middle; '3' = ring fingers). CC demands were manipulated by altering the composition of the number-sets: "congruent" trials featured the distinct number paired with zeros, which do not represent a response alternative, and spatially aligned with the corresponding response finger; conversely, "incongruent" trials featured both 'Flanker' interference introduced by distracter numbers (Eriksen and Eriksen, 1974) and 'Simon' conflict based on spatial incongruence between the target digit and the corresponding response finger (Simon and Berbaum, 1990). Working memory demands were introduced by requiring participants to withhold a response if the current 'distinct' number was the same as that presented '*n*' trials previously (where *n* represents the working memory load: 1 or 2). Two trials in which this condition was met were included in each working memory block.

The six conditions were presented in alternating blocks containing 8, 9, or 10 stimuli for 0-Back, 1-Back, and 2-Back blocks, respectively. The first stimulus in 1-Back blocks, and first two in 2-Back blocks were discarded during analysis to account for 'ramping-up' of WM load. Each stimulus was presented for 2 s and separated by variable inter-stimulus intervals of between 3.6 s and 7.2 s. Four blocks of each condition were presented across the experiment, each preceded by an instruction screen indicating the *n* of the subsequent block.

fMRI data acquisition

Images were obtained on a 3-Tesla Siemens Trio scanner equipped with a 32-channel head coil. Each functional run consisted of 354 whole-brain gradient-echo echo-planar (GRE-EPI) images composed of 36 interleaved, contiguous axial slices (TR = 2400 ms; TE = 32 ms; flip angle = 90°; slice thickness = 3 mm; in-plane resolution (matrix) = 3.3×3.3 mm (64×64); FOV = 210×210 mm). A high-resolution T1-weighted MPRAGE structural image was also acquired (176 sagittal slices; 0.9 mm isotropic voxels; TR = 1900 ms; TE = 2.24 ms; FOV = 230×230 mm; matrix = 256×256).

fMRI data analysis

Analysis was performed using SPM8 software (Functional Imaging Laboratory, UCL, UK). Structural (T1-weighted) images from each individual were first coregistered to the functional data and normalized to standard space (DARTEL; Ashburner, 2007). The estimated nonlinear transformation parameters were subsequently applied to the (rigid-body) motion-corrected functional data. The normalized data were interpolated to 2 mm isotropic voxels and spatially smoothed using a Gaussian kernel of 8 mm FWHM.

For each individual, the six task conditions were coded as individual predictors in a general linear model, alongside nuisance regressors accounting for error trials, instruction periods, and working memory ramping effects (i.e., first trial in 1-back blocks and first two trials in 2-back blocks). Each stimulus event was coded as a delta (i.e., stick) function and convolved with a canonical hemodynamic response function. Data were high-pass filtered (1/128 s), and temporal autocorrelations were estimated using a first-order autoregression model [AR(1)]. Parameters corresponding to each predictor were estimated using a restricted maximum likelihood approach. Contrast images were created among the six conditions of interest to infer the main positive effects of CC and WM (voxel-level family-wise error corrected $p < 0.05$) within a repeated-measures ANOVA framework.

Dynamic causal modeling

Deterministic, bilinear dynamic causal models (Friston et al., 2003) were used to assess large-scale neural interdependencies within the FPN using differential state equations comprised of three sets/matrices of parameters: *A*, context-invariant intrinsic influences between regions; *B*, context-dependent modulations of the intrinsic connections as a function of CC and WM demands; and *C*, exogenous visual inputs. Models of neuronal dynamics were combined with a hemodynamic model that describes the relationship between the (hidden) neuronal activity of the system and the measured fMRI signal (Friston et al., 2000). The parameters of the integrated model were estimated using a Bayesian inversion algorithm (Friston et al., 2003), as implemented in the DCM10 toolbox (Functional Imaging Laboratory, UCL, UK).

We tested a broad variety of models (see below). Estimates of the posterior evidence of these models were derived during Bayesian

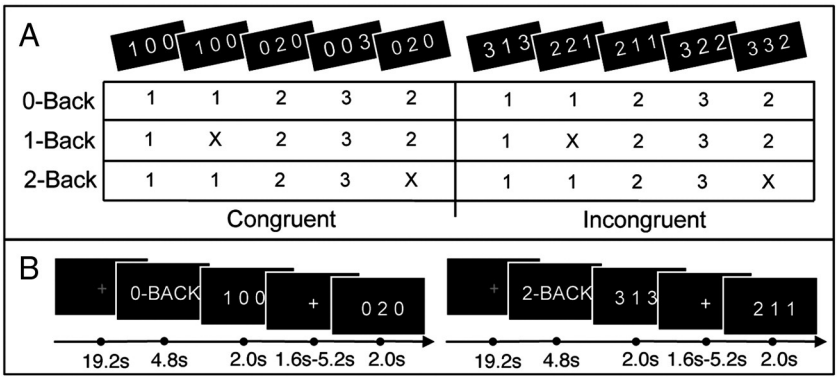

Fig. 1. *Experimental design. A*, 2 × 3 factorial structure of the cognitive paradigm with examples of visual stimuli corresponding to low-demand (congruent) and high-demand (incongruent) cognitive control presented at the top. Given a sequential presentation, the appropriate response option to each stimulus is indicated for the three levels of working memory demand. *B*, Example timecourse of experimental presentation, including rest periods (gray fixation) followed by an instruction screen and stimulus presentation with jittered interstimulus interval. Figure replicated from Harding et al. (in press).

inversion (Friston et al., 2007). Utilizing these estimates, group-level random-effects Bayesian Model Selection (rfx-BMS) was employed to infer the relative likelihood that a model, or family of models sharing a common characteristic, best represented the neural system at the population level (Penny et al., 2010; Stephan et al., 2009).

Network analysis overview

The overarching objective of this study was to disentangle the relative impact of WM and CC on interactions between a closely associated set of cortical brain regions that are collectively responsive to a broad range of higher-order cognitive manipulations (Cole and Schneider, 2007; Fedorenko et al., 2013; Niendam et al., 2012). These brain regions, representing the FPN, include the: (i) inferior frontal junction (IFJ), within the posterolateral prefrontal cortex; (ii) mid-dorsolateral prefrontal cortex (dlPFC); (iii) dorsomedial prefrontal cortex bridging the pre-supplementary motor area and dorsal anterior cingulate cortex (pSMA/dACC); and (iv) intraparietal sulcus (IPS) within the superior parietal cortex.

The number of ROIs included in network analyses was constrained by computational feasibility imposed by the extensive connectivity modeling approach employed (see below). Analyses were therefore restricted to a left-lateralized network, based on the relative weighting of task effects and greater consistency of individual-level activations within this hemisphere. In fact, individual-level activations in the right dlPFC and IFJ could not be reliably discriminated in all participants. Additionally, available evidence supports a left-lateralization of brain connectivity dynamics underlying language-based (versus spatial) cognitive tasks (Stephan et al., 2003).

Inference on network dynamics proceeded in a hierarchical fashion: First, the four regions forming the FPN (IFJ, dlPFC, pSMA/dACC, and IPS), as well as visual-perceptual areas, were identified in each individual. Second, inference was undertaken on task-dependent changes in bottom-up connectivity between the visual perceptual system and the cognitive FPN (i.e., perception–cognition interactions). Finally, task-dependent changes within the FPN were assessed. For computational feasibility, this step was initially undertaken on connections linking the IFJ, pSMA/dACC, and IPS; dlPFC interactions were then inferred.

This inference procedure corresponds to a greedy search of model space, similar to that applied in other DCM protocols, e.g., (Schlosser et al., 2010; Vossel et al., 2012). A greedy heuristic serves to approximate a global optimum solution by iteratively identifying local optima to subsets of the problem; each iteration builds on the previous step in a hierarchical fashion (Black, 2005). The greedy search employed here provides an approximation of optimal model structure while affording computational feasibility.

Region-of-interest (ROI) selection

The four ROIs forming the FPN (IFJ, dlPFC, pSMA/dACC, and IPS) were identified on the basis of the intersection (i.e., null conjunction) of the positive main effects of CC and WM (voxel-level FWE-corrected $p < 0.05$). In addition, a one-way ANOVA across all task conditions was used to localize peak activations related to perceptual processing in the visual cortex (V). Group activation foci served as a starting point to uniquely identify ROIs in each individual. For each individual, the global conjunction of the main CC and main WM effects was first calculated, and the peak-voxel nearest to the group-maximum of each ROI was identified. The first eigenvariate of the fMRI time-series was extracted from all voxels exceeding the uncorrected significance threshold of $p < 0.05$ within a 4 mm radius of the peak-voxel within each region. The timeseries were mean-centered and known variance of non-interest removed (e.g., task instruction periods; error trials).

Perception–cognition interactions: model specification and bayesian model selection

In this experiment, the FPN was differentially responsive to the presentation of the same visual stimulus as a function of changing CC and WM demands. It stands to reason that the influence of perceptual processes on at least one region of the FPN must therefore change in response to shifting cognitive demands, providing a mechanism for selective and flexible engagement of higher-order cognitive processes. In other words, the bottom-up connectivity between the visual system and the FPN must be sensitive to cognitive demand. However, cognitive engagement has been localized to each of the four regions of the FPN considered herein in previous works (c.f., Banich, 2009; Brass et al., 2005a; Carter and van Veen, 2007; Kravitz et al., 2011). We disambiguate this issue through the use of a model comparison approach.

First, we specified a model architecture in which stimulus presentation (i.e., the driving input, '*C*') elicited activity in the visual cortex. The driving input was not mean-centered in this study. Perceptual information subsequently propagated to each node of the FPN (i.e., through the unidirectional *A* matrix connectivity). Reciprocal interactions were included between the four regions of the FPN (i.e., a fully connected subgraph of the *A* matrix between these nodes; c.f. Fig. 3). This architecture was then modulated to variously model the influence of CC and WM demands on the magnitude of the bottom-up interactions between the perceptual system and the nodes of the FPN (i.e., the *B* matrix). Modulatory inputs were modeled as orthogonal main effects of CC or WM (i.e., Incongruent > Congruent; 2-Back > 0-Back). Specification of all possible combinations of CC and/or WM acting to modulate any or all of these connections resulted in 256 model architectures, which were

subsequently estimated for each participant. As significant WM × CC interaction effects were not evident in FPN fMRI activations (Harding et al., in press), interaction-related connectivity dynamics were not considered.

Family rfx-BMS analysis was performed to infer the most likely model structure at each of the four bottom-up connections (Penny et al., 2010). Each of the 256 models was assigned to one of four 'families' based on the task effects at, for example, the V → IFJ interaction: i) no modulation, ii) CC only, iii) WM only, or iv) both CC and WM. Each family contained 64 models. As each family collectively differed only in the task-sensitivity of this one connection, pooled evidence in favor of the different modulatory configurations could be robustly estimated while integrating over the effect of all other parameters in the models (Penny et al., 2010). The optimal model structure was inferred based on estimated exceedance probabilities (x_p), which represent the likelihood that each family had superior evidence to all others (Stephan et al., 2009). This process was replicated across each of the four bottom-up connections.

FPN connectivity: model specification and Bayesian model selection

The FPN is thought to adaptively encode representations of both CC and WM (Duncan, 2001; Harding et al., in press). However, in order for a common neuronal substrate to flexibly encapsulate diverse information, the system must be differentially tuned across changing contexts or goals. Differential interactions within this network may provide one mechanism underlying such context-specific encoding. To comprehensively test this idea, context-sensitive changes within the FPN were inferred in a comparable manner to perception–cognition interactions (above).

Due to computational demands, connectivity between the four network nodes (necessitating estimation of 4^{12} [>16 million] models) could not be considered in one step. On the basis of current theory, which highlights the importance of medial–lateral PFC dynamics to CC (e.g., Schlosser et al., 2010), and fronto-parietal dynamics to WM (e.g., Deserno et al., 2012), interactions between one node of the lateral PFC, the pSMA/dACC, and the IPS were first assessed. As the principle site of FPN engagement (see below), inclusion of the IFJ (as opposed to the dlPFC) was investigated in the first instance.

All possible combinations of CC and WM acting at each of the six reciprocal interactions between the IFJ, pSMA/dACC, and IPS were first defined, resulting in 4096 model architectures, and estimated for each individual. For each of the six connections, the 4096 models were evenly partitioned into the same four families as above (no modulation, CC only, WM only, both CC and WM) and rfx-BMS inference was undertaken. This procedure was then repeated for the six reciprocal interactions between the dlPFC and the other three nodes, requiring specification and estimation of a further 4096 models per subject.

The estimation of a large, comprehensive model space eschews specific assumptions regarding model structure, and eliminates reliance on a single architecture for inference of neural dynamics, providing for more robust assessment of network characteristics (Penny et al., 2010). This procedure is particularly useful in the present setting where prior evidence provides little definitive guidance to specifying particular models due to a lack of clear consensus opinion, e.g., (Banich, 2009; Carter and van Veen, 2007).

FPN connectivity: Bayesian Model Averaging

Following specification of a likely modulatory structure at each of the 12 connections within the FPN, quantification and inference on the parameter magnitudes was undertaken. Using a random-effects Bayesian Model Averaging approach, the posterior distributions of the parameter magnitudes at each connection across all participants and all models within the most likely model-family were estimated, with the contribution of each model weighted by its relative model evidence (Penny et al., 2010). The probability that the parameter magnitude differed from zero was assessed based on the proportion of the posterior distribution that lay above (or below) zero. A 95% posterior probability threshold was employed for reporting significance. This approach is roughly analogous to a one-tailed frequentist threshold of $p < 0.05$, in which the reported p-value is based on the proportion of the normal distribution that is more extreme than the estimated parameter. In both cases, probability is based on the size of the 'tail' of the distribution (e.g., Fig. 7B and 9B in Stephan et al., 2008). Using a Bayesian approach, inference is conditional on the estimated distribution of the actual data (which is approximately normally distributed), as opposed to a proposed 'null' distribution centered around zero. While the theoretical conceptualizations underlying the two approaches are distinct, they will yield roughly the same outcome in this instance, with distinctions primarily driven by deviations from exact normality in the data.

Results

Task-related fMRI activations and behavior

The null conjunction of the group-level main CC and main WM effects identified robust (FWE-corrected, voxel-level $p < 0.05$), spatially-coincident activations in each of the four ROIs selected to represent the left FPN (Fig. 2): IFJ (group MNI coordinates: x, y, z = −42, 4, 28); dlPFC (−38, 30, 18); pSMA/dACC (0, 16, 46); and IPS (−30, −54, 48); see Harding et al. (in press) for full, whole-brain results. No interaction effects between the two cognitive contexts were in evidence. The one-way ANOVA across all conditions additionally identified widespread activity in the visual cortex, centered (in the left-hemisphere) at MNI coordinates x, y, z = −26, −90, −2.

Similarly, a repeated-measures ANOVA of reaction times revealed significant main effects of both CC ($F_{1,24} = 194.5$, $p < 0.001$) and WM ($F_{2,48} = 120.9$, $p < 0.001$), but failed to support the presence of an interaction between the two ($F_{(2,48)} = 1.51$, $p = 0.23$). Comparable results were apparent with respect to error rates: both CC ($Z = -2.24$, $p = 0.03$) and WM ($Z = -3.93$, $p < 0.001$) elicited significant main effects, but no significant interaction was evident ($Z = -0.75$, $p = 0.45$). See Harding et al. (in press) for full behavioral results.

Perception–cognition interactions

The investigation of interactions between the visual cortex and FPN using family rfx-BMS indicated that both CC and WM likely modulated the influence of perceptual activity on the IFJ ($x_p = 0.72$). The effective connections from the visual cortex to the other three nodes of the FPN remained context-insensitive ($x_p > 0.93$; Fig. 3).

It is important to note that, as a random-effects analysis, this result represents a weighted effect across models and participants. As such,

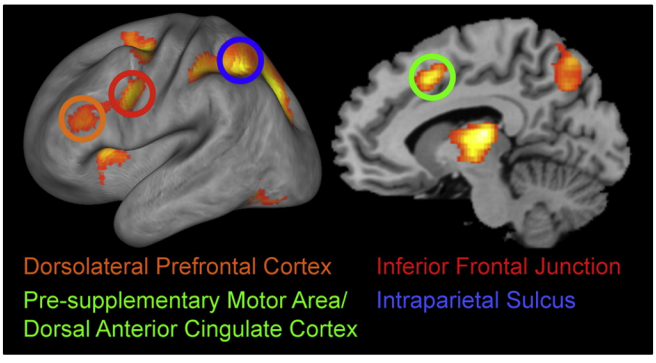

Fig. 2. *Task-related regions-of-interest.* The group-level null conjunction of the main positive cognitive control and working memory fMRI effects (FWE-corrected $p < 0.05$) highlights spatially coincident neural activations. Regions representing the frontoparietal control network are indicated.

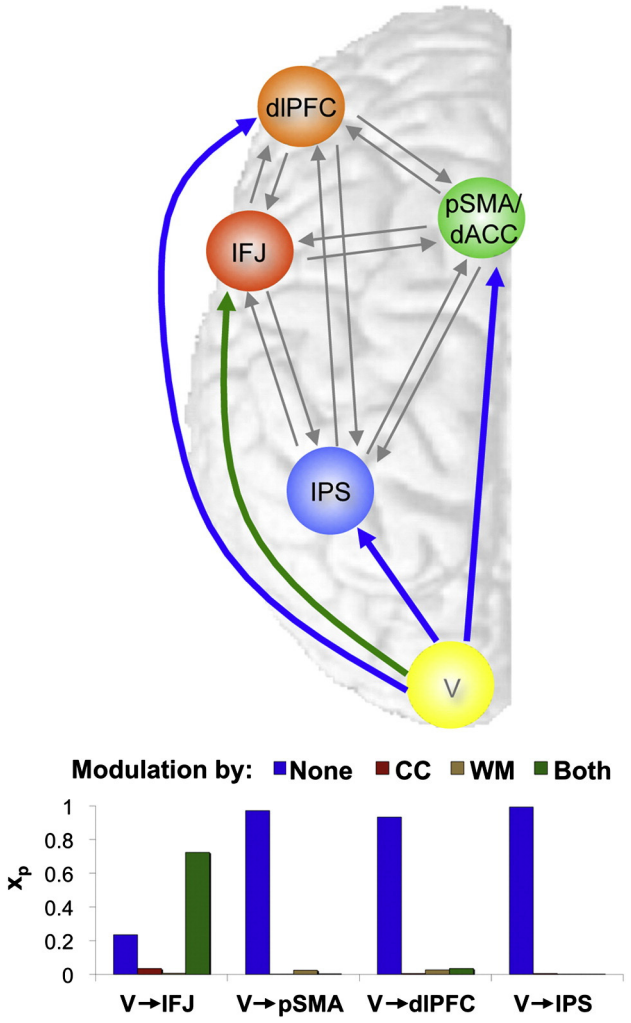

Fig. 3. *Perception–cognition interactions.* The most probable network structure governing the influence of the visual cortex on the frontoparietal network (FPN) is depicted (top) based on family Bayesian Model Selection (bottom; x_p = exceedance probability). All possible configurations of cognitive control (CC) and working memory (WM) acting on bottom-up influences (blue/green arrows) were compared. At this stage, interactions within the FPN (gray arrows) are held constant. V = visual cortex; dlPFC = dorsolateral prefrontal cortex; IFJ = inferior frontal cortex; pSMA/dACC = pre-supplementary motor area/dorsal anterior cingulate cortex; IPS = intraparietal sulcus.

more subtle effects specific to individual models or participants may be integrated out of consideration. This result was therefore further investigated by contrasting evidence in favor of each of the 256 individual models; that is, instead of pooling evidence across a number of models that share a common feature, all models were individually compared against all others. The single model in which CC and WM acted to modulate the interaction between the visual cortex and the IFJ was also found to have the greatest likelihood (Table 1). However, several other models also had appreciable relative model evidence. Therefore, while there is robust and reliable evidence in favor of the IFJ as a candidate site of FPN engagement, this analysis cannot rule out the additional, more circumscribed involvement of other network nodes in mediating perception–cognition interactions.

To simplify models used to study contextual effects within the FPN and to reduce computational burden, the visual cortex was removed in subsequent steps and the exogenous driving input mapped directly onto the IFJ (c.f., Stephan et al., 2010). For validation, the 15 possible driving input configurations by which a single input vector could act at any of the four FPN regions (i.e., all combinations, with the exception of no input) were specified and estimated for each participant. BMS

Table 1
Top 10 (of 256) perception–cognition interaction models.

Rank	Modulation of visual cortex to:				x_p
	SMA	IFJ	dlPFC	IPS	
1		CC, WM			0.079
2			WM		0.054
3	WM		CC		0.031
4			CC, WM		0.019
5	CC, WM				0.016
6				CC	0.015
7					0.015
8	WM	CC, WM			0.010
9		CC		WM	0.009
10		CC	CC, WM		0.007

CC = cognitive control; WM = working memory; x_p = exceedance probability.

provided corroborating evidence that the IFJ was indeed the most likely site of initial network engagement (x_p = 0.49; Table 2).

FPN connectivity: model selection

Estimated exceedance probabilities at each of the 12 interactions within the FPN provided clear evidence in favor of one likely model structure at all connections, with the exception of the influence of the pSMA/dACC on the IPS (Fig. 4). A further analysis was therefore performed to disambiguate the result at this connection, as follows: As opposed to dividing the model space into four equal families (see above), which allows for simultaneous inference on CC and WM, the influence of the two contexts were instead tested independently by dividing the full model space of 4096 structures into two families: i) modulation by CC at this connection, ii) no modulation by CC. This process was then repeated for WM. Evidence from all models in which CC acted to modulate this connection was found to be superior to those where it did not (x_p = 0.76), while the opposite was true of WM (x_p = 0.07). As such, the marginally winning family in the 4-partition analysis (modulated by CC only) was corroborated.

In summary, as depicted in Fig. 4, both CC and WM were found to likely modulate the influence of the IFJ and the IPS on the pSMA/dACC. Changes in effective connectivity were more extensive for CC than for WM. CC-unique modulations included outgoing connectivity from the pSMA/dACC to the IFJ and the IPS, as well as the inputs into the IFJ from the IPS and dlPFC. Modulations specific to WM were limited to the influence of the dlPFC on the pSMA/dACC. Interestingly, while

Table 2
Driving inputs into the frontoparietal network.

Rank	Driving inputs				x_p
	SMA	IFJ	dlPFC	IPS	
1		X			0.494
2			X		0.302
3				X	0.096
4	X				0.035
5		X		X	0.028
6		X	X		0.012
7	X	X			0.011
8			X	X	0.005
9	X			X	0.004
10	X		X		0.004
11	X	X		X	0.004
12		X	X	X	0.002
13	X	X	X		0.002
14	X		X	X	0.001
15	X	X	X	X	0.001

'X' indicates the inclusion of a driving input into the indicated region; x_p = exceedance probability.

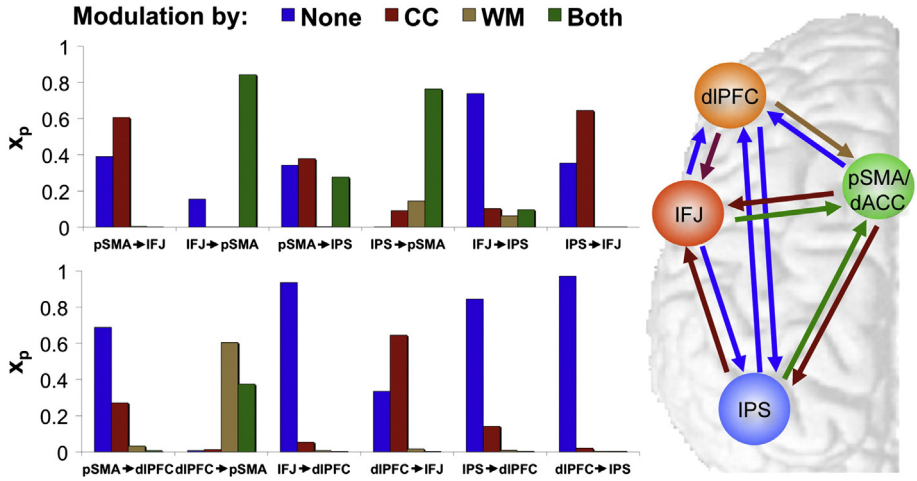

Fig. 4. *Bayesian model selection: frontoparietal dynamics.* The most probable network structure governing task-related modulation of interactions within the frontoparietal network (right), based on family Bayesian Model Selection (left; x_p = exceedance probability). All possible configurations of cognitive control (CC) and working memory (WM) acting on each connection were compared. Model selection was performed independently at each connection to derive a composite model. dlPFC = dorsolateral prefrontal cortex; IFJ = inferior frontal cortex; pSMA/dACC = pre-supplementary motor area/dorsal anterior cingulate cortex; IPS = intraparietal sulcus.

both contexts altered the sensitivity of the pSMA/dACC to nearly all inputs in this region, CC alone elicited the same effect at the IFJ. With the exception of the influence of the pSMA/dACC on the IPS, the strength of all inputs into the dlPFC and IPS were task-independent.

The process of interrogating the network through independent inference at each connection was supplemented by comparing model evidence across the 4096 individual model structures (at both the 1st and 2nd steps of the heuristic). The estimated exceedance probabilities assigned to any individual model were negligible in most cases, with even the top-ranked models reaching a probability of less than 0.003 of optimally representing the data, as compared to all other models. This finding is expected, given the diffusion of model-probability across the very large model space (i.e., chance probability = 1/4096 = 0.00024) and is one of the major factors motivating the use of family-level inference (Penny et al., 2010; Stephan et al., 2010). However, there are still a small number of models for which the evidence in their favor is appreciably larger than the vast majority of other structures. Although these models cannot be reliably discriminated based on their estimated exceedance probabilities alone, the composite models inferred based on family-level model comparison were found to conform to individual models found in the top 5 (of 4096) when evidence-ranked in their own right.

While the family-level inference approach allowed for robust comparison of CC and WM effects at each connection, this approach is insensitive to potential interactions between modulations across the network. As such, while the composite model (Fig. 4) represents valid outcomes for each connection independently, it may not fully encapsulate the nature of the network as an integrated system. Conversely, although model-level comparison considers the properties of the full network, definitive inference is not possible due to the dispersion of individual model evidences across the model space, as described above. We therefore also undertook an intermediate approach whereby the input/output structure of each region was assessed, and inference was performed separately for each of CC and WM (*Supplementary Information*). These analyses largely corroborated the structure of the composite network, suggesting that the impact of context on each connection largely outweighs the influence of any interactions among the modulatory parameters (Figure S1). However, inconsistencies between family-level and region-level analyses on IFJ-IPS modulation by CC do point to important interdependencies that may be evident along this axis. Disambiguation may require network description below the scale of family-level inference.

FPN connectivity: parameter inference

BMA across the models within the family having the highest likelihood at each connection revealed that the magnitude of the task-*independent* (i.e., "baseline"; *A* matrix) efferents from the IFJ and pSMA/dACC were significantly positive in all cases (Fig. 5; Table 3). The influence of the dlPFC on the IFJ was also positive, while a negative influence of the dlPFC was found to act on the IPS, although this latter finding was the weakest in magnitude by an appreciable margin. Notably, all efferents from the IPS failed to reach significance threshold, suggesting a largely anterior-to-posterior flow of information, while bi-directional interactions between frontal regions were nearly ubiquitous.

With respect to task-*dependent* dynamics (i.e., *B* matrix), both CC and WM demands were found to further increase the facilitatory influence of the IFJ on the pSMA/dACC and to introduce a negative influence of the IPS on the pSMA/dACC (Fig. 5; Table 3). CC alone also induced enhancements of the positive connectivity between the pSMA/dACC and the IPS, and the dlPFC to the IFJ; a trend-level (p = 92%) reduction in the influence of the pSMA/dACC on the IFJ as also observed. WM acted uniquely to introduce a negative modulation of the influence of the dlPFC on the pSMA/dACC.

All modulatory effects identified during model-space inference (above) were found to have significantly non-zero magnitudes, with the exception of the impact of CC on IPS-to-IFJ connectivity and the trend-level result reported immediately previous. The influence of CC on IPS-IFJ interactions was also inconclusive in region-based analysis of network function (*Supplementary Information*). Interestingly, the absence of the IPS-to-IFJ modulation yields the individual model structure having the highest evidence based on model-level BMS. This result suggests that while the modulation of IPS-to-IFJ connectivity is more representative of the data when integrating out all other network properties, its absence is more likely when considering the unique dependencies of an individual network structure. Taken together, the application of a combined model-space and parameter-space family-level inference procedure, in addition to model-level and region-level inference, provide confidence in the inferred model structure.

Discussion

This study provides novel insights into the shared and unique properties of functional integration underlying CC and WM within a

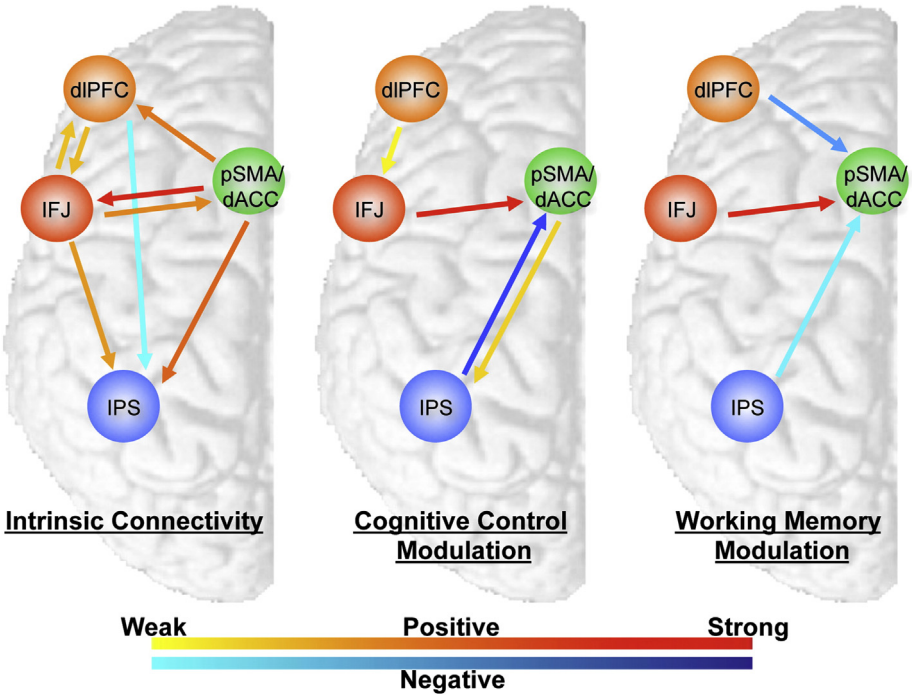

Fig. 5. *Frontoparietal effective connectivity.* Significant (>95% posterior probability) task-independent intrinsic interactions (left), cognitive control related modulations (center), and working memory related modulations (right), based on Bayesian Model Averaging. Color gradients represent parameter magnitudes and are scaled independently for each set of results; see Table 3 for empirical values.

common network of higher-order cortical regions. While many properties of the FPN were shared across CC and WM contexts, unique dynamics in effective connectivity were also found to discriminate these processes. First, of the brain regions representing the FPN, inputs into the IFJ were found to be the most responsive to changes in cognitive demand, regardless of context, possibly serving to adaptively engage higher-order processes. Second, task-invariant (baseline) effective influences between prefrontal regions of the FPN were general bi-directional, while frontal-to-parietal interactions were hierarchical in nature. Finally, connectivity dynamics common to both contexts were evident at inputs into the pSMA/dACC, while CC additionally influenced rostral-to-caudal interactions within the lateral PFC and between the pSMA/dACC and IPS; WM-unique modulations were restricted to the influence of the dlPFC on the pSMA/dACC. Critically, network dynamics occur almost ubiquitously at interactions involving the pSMA/dACC, reflecting the core relevance of medial prefrontal interactions to the function and flexibility of the FPN during cognitive performance.

Table 3
Connectivity parameters.

Source	Target	Estimate	SD	p
Intrinsic connectivity				
IFJ	SMA	0.46	0.056	**1.00**
SMA	IFJ	0.78	0.052	**1.00**
IFJ	IPS	0.40	0.051	**1.00**
IPS	IFJ	−0.032	0.065	0.69
SMA	IPS	0.56	0.051	**1.00**
IPS	SMA	−0.059	0.065	0.82
dlPFC	SMA	−0.038	0.059	0.74
SMA	dlPFC	0.50	0.046	**1.00**
dlPFC	IFJ	0.31	0.056	**1.00**
IFJ	dlPFC	0.29	0.059	**1.00**
dlPFC	IPS	−0.10	0.056	**0.96**
IPS	dlPFC	−0.025	0.058	0.67
Cognitive control modulations				
IFJ	SMA	1.08	0.11	**1.00**
SMA	IFJ	−0.26	0.18	0.92
IPS	IFJ	0.030	0.17	0.58
SMA	IPS	0.46	0.21	**0.99**
IPS	SMA	−0.91	0.21	**1.00**
dlPFC	IFJ	0.34	0.16	**0.99**
Working memory modulations				
dlPFC	SMA	−1.32	0.14	**1.00**
IFJ	SMA	1.88	0.16	**1.00**
IPS	SMA	−0.95	0.15	**1.00**

Estimate = maximum *a posteriori* value of the posterior distribution (parameter magnitude estimate); SD = standard deviation; p = posterior probability; bold entries are significant at a threshold of p > 95%.

In line with current inference suggesting a primary role for the IFJ in engaging cognition, this region has been previously implicated in the encoding and updating of task-sets (e.g., targets of attention) relevant to current behavioral demands. Furthermore, this region sits at a nexus of bottom-up pathways governing stimulus-driven attention and top-down pathways supporting perceptual and behavioral control (Badre, 2008; Brass and von Cramon, 2004; Brass et al., 2005a; Corbetta and Shulman, 2002; Derrfuss et al., 2004; Derrfuss et al., 2005). Contextual ambiguity and response uncertainty inherent to our CC and WM manipulations may therefore trigger, or augment, task representations encoded in the IFJ.

It is relevant to note that the FPN does not receive direct afferents from the visual system. The bottom-up engagement of control resources in the IFJ instead likely occurs indirectly via the ventral attention/salience network, which includes regions of the temporo-parietal junction and the anterior insula (Corbetta and Shulman, 2002; Palaniyappan et al., 2013; Seeley et al., 2007; Vossel et al., 2012). Therefore, while visual perception occurs via a posterior-to-anterior processing stream (Kravitz et al., 2011), cognitive engagement instead relies on an indirect mechanism of prefrontal engagement which, in turn, feeds-back to posterior structures, consistent with classical "top-down" control models (Gazzaley and Nobre, 2012). This interpretation is also consistent with electrophysiological evidence suggesting an earlier engagement of frontal as compared to parietal activity related to cognitive control processes (Brass et al., 2005b; Gobbele et al., 2008; Grent-'t-Jong and Woldorff, 2007; Liotti et al., 2000); but see also (Green and McDonald, 2008).

Bi-directional, positive interactions between the three prefrontal regions of the FPN (IFJ, dlPFC, pSMA/dACC) were almost universally evident, irrespective of task context, suggesting a highly interactive "baseline" exchange of information between these regions. This finding is consistent with resting-state connectivity studies supporting tight functional integration between these regions (Raichle, 2011), and electrophysiological signals evidencing signal propagation in both directions along the medial–lateral axis of the prefrontal cortex, e.g., (Hanslmayr et al., 2008; Markela-Lerenc et al., 2004; Silton et al., 2010). On top of this foundation, variations in the strength of these interactions as a function of task demands were sparse, yet almost exclusively confined to interactions involving the pSMA/dACC. The robust upregulation of the influence of the IFJ on the pSMA/dACC by both CC and WM points to a common mechanism that may underlie initiation of action-selection, response preparation, outcome monitoring, and error prediction — processes localized to the pSMA/dACC (Alexander and Brown, 2011; Isoda and Hikosaka, 2007; Nachev et al., 2008; Rushworth et al., 2007) - in accordance with the context-relevant task-set represented in the IFJ (Brass et al., 2005a). Taken together, the engagement of the FPN via the lateral prefrontal cortex and the observed medial–lateral task-related dynamics within the network are broadly consistent with the 'cascade-of-control' model of behavioral control. This account posits that the postero-lateral PFC (i.e., IFJ) is responsible for creating and maintaining a task-relevant attentional set while downstream medial areas serve to gate/select between competing task responses and evaluate response outcomes (Banich, 2009; Silton et al., 2010). Our work hence lends weight to this model as a generalizable framework governing higher-order brain function.

Cognitive control demands were additionally associated with an upregulation of anterior-to-posterior connectivity within the lateral PFC, consistent with hierarchical models of control-related function along the rostro-causal axis of the PFC (Badre and D'Esposito, 2009; Koechlin and Summerfield, 2007). The dlPFC – the putative seat of sustained behavioral control and temporally-extended goal maintenance (Badre, 2008) – has been previously shown to dynamically bias more concrete and immediate task-sets in posterior areas, including the IFJ, as a function of control demands (Koechlin and Summerfield, 2007; Koechlin et al., 2003; Kouneiher et al., 2009). This effect may be specific to disambiguating competing stimulus–response tendencies or conflicting attentional sets, requirements specific to CC as compared to WM processes.

In contrast to the reciprocal interactions defining connectivity within the PFC, fronto-parietal interactions were hierarchical in nature and selectively gated by CC demands. While these interactions do not represent 'top-down' relationships *per se*, as all areas of the FPN lie within association cortices, this finding does suggest that the representation of behavioral goals and outcome contingencies in prefrontal regions may serve to bias context representations and stimulus–response associations encoded in the IPS (Bunge et al., 2002; Corbetta and Shulman, 2002; Rushworth et al., 2001); as before, WM processes may not require such arbitration. Notably, however, fronto-parietal connectivity dynamics related to WM processes have been reported in previous studies (Edin et al., 2009; Honey et al., 2002; Sauseng et al., 2005), including several recent DCM investigations (Deserno et al., 2012; Dima et al., 2014; Ma et al., 2012; Schmidt et al., 2014). However, consensus has not yet emerged regarding the direction (frontal-to-parietal, or vice versa), laterality, or specific source/target regions that underlie observed WM-related modulations. Differences among studies may be attributable to distinct model structures (e.g., inputs into parietal vs. frontal regions), heuristics employed to facilitate inference, or the inclusion of different sets of cortical regions in network models. While the current study does not provide evidence in favor of changes to prefrontal-superior parietal connectivity as a function of WM demands, this line of inquiry clearly requires further attention.

Finally, evidence of transient, task-related negative feedback from parietal and lateral prefrontal regions to the pSMA/dACC provides a putative mechanism for balancing the engagement of effortful cognitive resources, c.f., (Botvinick et al., 2001; MacDonald et al., 2000). As abstract task representations or sustained WM-related activity become established in the dlPFC, and context/intention maps in the IPS are augmented or updated in response to current demands, superordinate evaluative processes in the pSMA/dACC may, in turn, be damped. Taken alongside the observation that all but one of the identified task-related modulations of FPN connectivity involved the pSMA/dACC, these results support a central role for the medial prefrontal cortex in directing CC and WM processes in the brain.

Overall, this study builds substantially upon current knowledge regarding functional integration in the FPN through the use of a comprehensive modeling approach. By accruing evidence and undertaking inference across a large number of putative model structures, we eschew specific assumptions regarding network characteristics. The present results are therefore robust to the idiosyncrasies that may characterize individual models, providing for greater confidence when generalizing these results. Moreover, this work moves beyond pair-wise interactions along the medial–lateral and rostro–caudal axes of the PFC, as well as anterior–posterior interactions across the cortex, that have predominated neurobiological models of CC and WM to date. We have also employed an experimental task design that allows for direct comparison of unique cognitive demands on a common neural framework.

A number of limitations of the present study provide targets for future work. First, the network we characterized was limited to a few key regions. Future investigation of right-lateralized and inter-hemispheric interactions, as well as incorporation of other brain regions central to cognitive functioning, such as the anterior insula (Fan et al., 2014; Menon and Uddin, 2010), basal ganglia (Aron et al., 2007), and cerebellum (Georgiou-Karistianis et al., 2012) into modeling analyses may help further refine descriptions of relevant neural dynamics. The top-down influence of cognitive systems on perceptual, motor, limbic, and mnemonic functions also remains of great interest to the field of cognitive neuroscience (e.g., Feredoes et al., 2011; Zanto et al., 2011). Furthermore, while we have used well-established exemplars of CC and WM tasks, generalization of the current results to other behavioral demands and task contexts (e.g., response inhibition; spatial stimuli) will be essential for determining the task-general versus task-specific characteristics of dynamic FPN function. Finally, while family-level rfx-BMS provides for reliable and generalizable inference across models and individuals, more subtle properties of network function may be integrated out of consideration. We have mitigated this issue by performing inference across different network scales (i.e., individual connections; individual nodes; individual models). However, future work will be necessary to disambiguate the influence of more circumscribed network characteristics over and above the robust foundation established herein.

In sum, this work highlights shared and unique dynamics of the large-scale interconnectivity defining the FPN across distinct cognitive demands. Common connectivity dynamics may underlie the engagement of action selection and performance evaluation processes. Conversely, the need to augment task and context representations may be specific to reallocating cognitive resources (i.e., cognitive control), as compared to actively maintaining and manipulating information in mind (i.e., working memory). Such flexible functional integration may provide a mechanistic foundation that describes the adaptability of neural representations within this common system, underlining the extraordinary flexibility inherent to human cognition.

Acknowledgments

This study was supported by funding from the Australian National Health and Medical Research Council (Project Grant 1008921; Program Grant 566529; Clinical Career Development Fellowship 628509 to B.J.H.; Senior Principal Research Fellowship 628386 to C.P.; Senior Research

Fellowship 1021973 to M.Y.). The authors declare no competing financial interests.

Appendix A. Supplementary data

Supplementary data to this article can be found online at http://dx.doi.org/10.1016/j.neuroimage.2014.11.039.

References

Alexander, W.H., Brown, J.W., 2011. Medial prefrontal cortex as an action-outcome predictor. Nat. Neurosci. 14, 1338–1344.

Aron, A.R., Durston, S., Eagle, D.M., Logan, G.D., Stinear, C.M., Stuphorn, V., 2007. Converging evidence for a fronto–basal-ganglia network for inhibitory control of action and cognition. J. Neurosci. 27, 11860–11864.

Ashburner, J., 2007. A fast diffeomorphic image registration algorithm. Neuroimage 38, 95–113.

Baddeley, A., 2003. Working memory: looking back and looking forward. Nat. Rev. Neurosci. 4, 829–839.

Badre, D., 2008. Cognitive control, hierarchy, and the rostro–caudal organization of the frontal lobes. Trends Cogn. Sci. 12, 193–200.

Badre, D., D'Esposito, M., 2009. Is the rostro–caudal axis of the frontal lobe hierarchical? Nat. Rev. Neurosci. 10, 659–669.

Banich, M., 2009. Executive function: the search for an integrated account. Curr. Dir. Psychol. Sci. 18, 89–94.

Black, P.E., 2005. Greedy algorithm. In: Black, P.E. (Ed.), Dictionary of Algorithms and Data Structures. U.S. National Institute of Standards and Technology.

Botvinick, M.M., Braver, T.S., Barch, D.M., Carter, C.S., Cohen, J.D., 2001. Conflict monitoring and cognitive control. Psychol. Rev. 108, 624–652.

Brass, M., von Cramon, D.Y., 2004. Decomposing components of task preparation with functional magnetic resonance imaging. J. Cogn. Neurosci. 16, 609–620.

Brass, M., Derrfuss, J., Forstmann, B., von Cramon, D.Y., 2005a. The role of the inferior frontal junction area in cognitive control. Trends Cogn. Sci. 9, 314–316.

Brass, M., Ullsperger, M., Knoesche, T.R., von Cramon, D.Y., Phillips, N.A., 2005b. Who comes first? The role of the prefrontal and parietal cortex in cognitive control. J. Cogn. Neurosci. 17, 1367–1375.

Bunge, S.A., Hazeltine, E., Scanlon, M.D., Rosen, A.C., Gabrieli, J.D., 2002. Dissociable contributions of prefrontal and parietal cortices to response selection. Neuroimage 17, 1562–1571.

Bush, G., Shin, L.M., 2006. The multi-source interference task: an fMRI task that reliably activates the cingulo–frontal–parietal cognitive/attention network. Nat. Protoc. 1, 308–313.

Carter, C.S., van Veen, V., 2007. Anterior cingulate cortex and conflict detection: an update of theory and data. Cogn. Affect. Behav. Neurosci. 7, 367–379.

Cieslik, E.C., Zilles, K., Grefkes, C., Eickhoff, S.B., 2011. Dynamic interactions in the fronto-parietal network during a manual stimulus–response compatibility task. Neuroimage 58, 860–869.

Cocchi, L., Zalesky, A., Fornito, A., Mattingley, J.B., 2013. Dynamic cooperation and competition between brain systems during cognitive control. Trends Cogn. Sci. 17, 493–501.

Cole, M.W., Schneider, W., 2007. The cognitive control network: integrated cortical regions with dissociable functions. Neuroimage 37, 343–360.

Cole, M.W., Reynolds, J.R., Power, J.D., Repovs, G., Anticevic, A., Braver, T.S., 2013. Multi-task connectivity reveals flexible hubs for adaptive task control. Nat. Neurosci. 16, 1348–1355.

Corbetta, M., Shulman, G.L., 2002. Control of goal-directed and stimulus-driven attention in the brain. Nat. Rev. Neurosci. 3, 201–215.

Daunizeau, J., David, O., Stephan, K.E., 2011. Dynamic causal modelling: a critical review of the biophysical and statistical foundations. Neuroimage 58, 312–322.

Derrfuss, J., Brass, M., von Cramon, D.Y., 2004. Cognitive control in the posterior frontolateral cortex: evidence from common activations in task coordination, interference control, and working memory. Neuroimage 23, 604–612.

Derrfuss, J., Brass, M., Neumann, J., von Cramon, D.Y., 2005. Involvement of the inferior frontal junction in cognitive control: meta-analyses of switching and Stroop studies. Hum. Brain Mapp. 25, 22–34.

Deserno, L., Sterzer, P., Wustenberg, T., Heinz, A., Schlagenhauf, F., 2012. Reduced prefrontal-parietal effective connectivity and working memory deficits in schizophrenia. J. Neurosci. 32, 12–20.

Dima, D., Jogia, J., Frangou, S., 2014. Dynamic causal modeling of load-dependent modulation of effective connectivity within the verbal working memory network. Hum. Brain Mapp. 35, 3025–3035.

Dosenbach, N.U., Fair, D.A., Cohen, A.L., Schlaggar, B.L., Petersen, S.E., 2008. A dual-networks architecture of top-down control. Trends Cogn. Sci. 12, 99–105.

Duncan, J., 2001. An adaptive coding model of neural function in prefrontal cortex. Nat. Rev. Neurosci. 2, 820–829.

Edin, F., Klingberg, T., Johansson, P., McNab, F., Tegner, J., Compte, A., 2009. Mechanism for top-down control of working memory capacity. Proc. Natl. Acad. Sci. U. S. A. 106, 6802–6807.

Eriksen, B.A., Eriksen, C.W., 1974. Effects of noise letters upon the identification of a target letter in a nonsearch task. Atten. Percept. Psychophys. 16, 143–149.

Fan, J., Hof, P.R., Guise, K.G., Fossella, J.A., Posner, M.I., 2008. The functional integration of the anterior cingulate cortex during conflict processing. Cereb. Cortex 18, 796–805.

Fan, J., Van Dam, N.T., Gu, X., Liu, X., Wang, H., Tang, C.Y., Hof, P.R., 2014. Quantitative characterization of functional anatomical contributions to cognitive control under uncertainty. J. Cogn. Neurosci. 26, 1490–1506.

Fedorenko, E., Duncan, J., Kanwisher, N., 2013. Broad domain generality in focal regions of frontal and parietal cortex. Proc. Natl. Acad. Sci. U. S. A. 110, 16616–16621.

Feredoes, E., Heinen, K., Weiskopf, N., Ruff, C., Driver, J., 2011. Causal evidence for frontal involvement in memory target maintenance by posterior brain areas during distracter interference of visual working memory. Proc. Natl. Acad. Sci. U. S. A. 108, 17510–17515.

First, M.B., Spitzer, R.L., Gibbon, M., Williams, J.B., 2002. Structured Clinical Interview for DSM-IV-TR Axis I Disorders, Research Version, Non-patient Edition. Biometrics Research, New York State Psychiatric Institute, New York.

Friston, K.J., 2011. Functional and effective connectivity: a review. Brain Connect. 1, 13–36.

Friston, K.J., Mechelli, A., Turner, R., Price, C.J., 2000. Nonlinear responses in fMRI: the Balloon model, Volterra kernels, and other hemodynamics. Neuroimage 12, 466–477.

Friston, K.J., Harrison, L., Penny, W., 2003. Dynamic causal modelling. Neuroimage 19, 1273–1302.

Friston, K., Mattout, J., Trujillo-Barreto, N., Ashburner, J., Penny, W., 2007. Variational free energy and the Laplace approximation. Neuroimage 34, 220–234.

Friston, K., Moran, R., Seth, A.K., 2013. Analysing connectivity with Granger causality and dynamic causal modelling. Curr. Opin. Neurobiol. 23, 172–178.

Gazzaley, A., Nobre, A.C., 2012. Top-down modulation: bridging selective attention and working memory. Trends Cogn. Sci. 16, 129–135.

Georgiou-Karistianis, N., Akhlaghi, H., Corben, L.A., Delatycki, M.B., Storey, E., Bradshaw, J.L., Egan, G.F., 2012. Decreased functional brain activation in Friedreich ataxia using the Simon effect task. Brain Cogn. 79, 200–208.

Gobbele, R., Lamberty, K., Stephan, K.E., Stegelmeyer, U., Buchner, H., Marshall, J.C., Fink, G.R., Waberski, T.D., 2008. Temporal activation patterns of lateralized cognitive and task control processes in the human brain. Brain Res. 1205, 81–90.

Green, J.J., McDonald, J.J., 2008. Electrical neuroimaging reveals timing of attentional control activity in human brain. PLoS Biol. 6, e81.

Grent-'t-Jong, T., Woldorff, M.G., 2007. Timing and sequence of brain activity in top-down control of visual–spatial attention. PLoS Biol. 5, e12.

Hanslmayr, S., Pastotter, B., Bauml, K.H., Gruber, S., Wimber, M., Klimesch, W., 2008. The electrophysiological dynamics of interference during the Stroop task. J. Cogn. Neurosci. 20, 215–225.

Harding, I.H., Harrison, B.J., Breakspear, M., Pantelis, C., Yucel, M., 2014. Cortical representations of cognitive control and working memory are dependent yet non-interacting. Cereb. Cortex (in press).

Honey, G.D., Fu, C.H., Kim, J., Brammer, M.J., Croudace, T.J., Suckling, J., Pich, E.M., Williams, S.C., Bullmore, E.T., 2002. Effects of verbal working memory load on corticocortical connectivity modeled by path analysis of functional magnetic resonance imaging data. Neuroimage 17, 573–582.

Isoda, M., Hikosaka, O., 2007. Switching from automatic to controlled action by monkey medial frontal cortex. Nat. Neurosci. 10, 240–248.

Kadohisa, M., Petrov, P., Stokes, M., Sigala, N., Buckley, M., Gaffan, D., Kusunoki, M., Duncan, J., 2013. Dynamic construction of a coherent attentional state in a prefrontal cell population. Neuron 80, 235–246.

Koechlin, E., Summerfield, C., 2007. An information theoretical approach to prefrontal executive function. Trends Cogn. Sci. 11, 229–235.

Koechlin, E., Ody, C., Kouneiher, F., 2003. The architecture of cognitive control in the human prefrontal cortex. Science 302, 1181–1185.

Kouneiher, F., Charron, S., Koechlin, E., 2009. Motivation and cognitive control in the human prefrontal cortex. Nat. Neurosci. 12, 939–945.

Kravitz, D.J., Saleem, K.S., Baker, C.I., Mishkin, M., 2011. A new neural framework for visuospatial processing. Nat. Rev. Neurosci. 12, 217–230.

Liotti, M., Woldorff, M.G., Perez, R., Mayberg, H.S., 2000. An ERP study of the temporal course of the Stroop color-word interference effect. Neuropsychologia 38, 701–711.

Ma, L., Steinberg, J.L., Hasan, K.M., Narayana, P.A., Kramer, L.A., Moeller, F.G., 2012. Working memory load modulation of parieto-frontal connections: evidence from dynamic causal modeling. Hum. Brain Mapp. 33, 1850–1867.

MacDonald III, A.W., Cohen, J.D., Stenger, V.A., Carter, C.S., 2000. Dissociating the role of the dorsolateral prefrontal and anterior cingulate cortex in cognitive control. Science 288, 1835–1838.

Markela-Lerenc, J., Ille, N., Kaiser, S., Fiedler, P., Mundt, C., Weisbrod, M., 2004. Prefrontal–cingulate activation during executive control: which comes first? Brain Res. Cogn. Brain Res. 18, 278–287.

Menon, V., Uddin, L.Q., 2010. Saliency, switching, attention and control: a network model of insula function. Brain Struct. Funct. 214, 655–667.

Nachev, P., Kennard, C., Husain, M., 2008. Functional role of the supplementary and pre-supplementary motor areas. Nat. Rev. Neurosci. 9, 856–869.

Niendam, T.A., Laird, A.R., Ray, K.L., Dean, Y.M., Glahn, D.C., Carter, C.S., 2012. Meta-analytic evidence for a superordinate cognitive control network subserving diverse executive functions. Cogn. Affect. Behav. Neurosci. 12, 241–268.

Palaniyappan, L., Simmonite, M., White, T.P., Liddle, E.B., Liddle, P.F., 2013. Neural primacy of the salience processing system in schizophrenia. Neuron 79, 814–828.

Penny, W.D., Stephan, K.E., Daunizeau, J., Rosa, M.J., Friston, K.J., Schofield, T.M., Leff, A.P., 2010. Comparing families of dynamic causal models. PLoS Comput. Biol. 6, e1000709.

Power, J.D., Cohen, A.L., Nelson, S.M., Wig, G.S., Barnes, K.A., Church, J.A., Vogel, A.C., Laumann, T.O., Miezin, F.M., Schlaggar, B.L., Petersen, S.E., 2011. Functional network organization of the human brain. Neuron 72, 665–678.

Prado, J., Carp, J., Weissman, D.H., 2011. Variations of response time in a selective attention task are linked to variations of functional connectivity in the attentional network. Neuroimage 54, 541–549.

Raichle, M.E., 2011. The restless brain. Brain Connect. 1, 3–12.

Rushworth, M.F., Paus, T., Sipila, P.K., 2001. Attention systems and the organization of the human parietal cortex. J. Neurosci. 21, 5262–5271.
Rushworth, M.F., Buckley, M.J., Behrens, T.E., Walton, M.E., Bannerman, D.M., 2007. Functional organization of the medial frontal cortex. Curr. Opin. Neurobiol. 17, 220–227.
Sauseng, P., Klimesch, W., Schabus, M., Doppelmayr, M., 2005. Fronto-parietal EEG coherence in theta and upper alpha reflect central executive functions of working memory. Int. J. Psychophysiol. 57, 97–103.
Schlosser, R.G., Wagner, G., Koch, K., Dahnke, R., Reichenbach, J.R., Sauer, H., 2008. Fronto-cingulate effective connectivity in major depression: a study with fMRI and dynamic causal modeling. Neuroimage 43, 645–655.
Schlosser, R.G., Wagner, G., Schachtzabel, C., Peikert, G., Koch, K., Reichenbach, J.R., Sauer, H., 2010. Fronto-cingulate effective connectivity in obsessive compulsive disorder: a study with fMRI and dynamic causal modeling. Hum. Brain Mapp. 31, 1834–1850.
Schmidt, A., Smieskova, R., Simon, A., Allen, P., Fusar-Poli, P., McGuire, P.K., Bendfeldt, K., Aston, J., Lang, U.E., Walter, M., Radue, E.W., Riecher-Rossler, A., Borgwardt, S.J., 2014. Abnormal effective connectivity and psychopathological symptoms in the psychosis high-risk state. J. Psychiatry Neurosci. 39, 130102.
Seeley, W.W., Menon, V., Schatzberg, A.F., Keller, J., Glover, G.H., Kenna, H., Reiss, A.L., Greicius, M.D., 2007. Dissociable intrinsic connectivity networks for salience processing and executive control. J. Neurosci. 27, 2349–2356.
Silton, R.L., Heller, W., Towers, D.N., Engels, A.S., Spielberg, J.M., Edgar, J.C., Sass, S.M., Stewart, J.L., Sutton, B.P., Banich, M.T., Miller, G.A., 2010. The time course of activity in dorsolateral prefrontal cortex and anterior cingulate cortex during top-down attentional control. Neuroimage 50, 1292–1302.
Simon, J.R., Berbaum, K., 1990. Effect of conflicting cues on information processing: the 'Stroop effect' vs. the 'Simon effect'. Acta Psychol. (Amst) 73, 159–170.
Stephan, K.E., Marshall, J.C., Friston, K.J., Rowe, J.B., Ritzl, A., Zilles, K., Fink, G.R., 2003. Lateralized cognitive processes and lateralized task control in the human brain. Science 301, 384–386.
Stephan, K.E., Kasper, L., Harrison, L.M., Daunizeau, J., den Ouden, H.E.M., Breakspear, M., Friston, K.J., 2008. Nonlinear dynamic causal models for fMRI. Neuroimage 42, 649–662.
Stephan, K.E., Penny, W.D., Daunizeau, J., Moran, R.J., Friston, K.J., 2009. Bayesian model selection for group studies. Neuroimage 46, 1004–1017.
Stephan, K.E., Penny, W.D., Moran, R.J., den Ouden, H.E., Daunizeau, J., Friston, K.J., 2010. Ten simple rules for dynamic causal modeling. Neuroimage 49, 3099–3109.
Stokes, M.G., Kusunoki, M., Sigala, N., Nili, H., Gaffan, D., Duncan, J., 2013. Dynamic coding for cognitive control in prefrontal cortex. Neuron 78, 364–375.
Vossel, S., Weidner, R., Driver, J., Friston, K.J., Fink, G.R., 2012. Deconstructing the architecture of dorsal and ventral attention systems with dynamic causal modeling. J. Neurosci. 32, 10637–10648.
Wang, L., Liu, X., Guise, K.G., Knight, R.T., Ghajar, J., Fan, J., 2010. Effective connectivity of the fronto-parietal network during attentional control. J. Cogn. Neurosci. 22, 543–553.
Wechsler, D., 1999. Wechsler Abbreviated Scale of Intelligence Manual. The Psychological Corporation, San Antonio.
Zanto, T.P., Rubens, M.T., Thangavel, A., Gazzaley, A., 2011. Causal role of the prefrontal cortex in top-down modulation of visual processing and working memory. Nat. Neurosci. 14, 656–661.